JOURNAL OF Materials CHEMISTRY

Synthesis of TOPO-capped Mn-doped ZnS and CdS quantum dots

M. Azad Malik,[a] Paul O'Brien*[b] and N. Revaprasadu[c]

[a]*Department of Chemistry, Imperial College of Science, Technology and Medicine, South Kensington, London, UK SW7 2AZ*
[b]*The Manchester Materials Science Centre and the Department of Chemistry, University of Manchester, Oxford Rd, Manchester, UK M13 9PL. E-mail: paul.obrien@man.ac.uk*
[c]*Department of Chemistry, University of Zululand, Private Bag X1001, Kwadlangezwa 3886, South Africa*

Received 23rd March 2001, Accepted 1st June 2001
First published as an Advance Article on the web 26th July 2001

TOPO (tri-*n*-octylphosphine oxide) capped Mn-doped ZnS and Mn-doped CdS nanoparticles have been prepared from bis(diethyldithiocarbamato)zinc(II) or bis(methylhexyldithiocarbamato)cadmium(II) and manganese dichloride. The nanoparticles obtained all show quantum size effects in their optical spectra with respect to the parent CdS and ZnS.

There are clear differences in the photoluminescence of the ZnS (448 nm) and ZnS : Mn (510 nm) samples. The level of Mn-doping can be differentiated by the photoluminescence intensity, all of the doped samples show an emission maximum at 510 nm. EPR spectra and ICP results confirm the quantitative incorporation of manganese into the ZnS quantum dots. Selected area electron diffraction (SAED), X-ray diffraction (XRD) and transmission electron microscopy (TEM) show the material to be hexagonal. The crystallinity of the material was also evident from high resolution transmission electron microscopy (HRTEM) which gave well-defined images of particles with clear lattice fringes.

The PL spectrum of the doped CdS nanoparticles has an emission maximum at 585 nm as is usually attributed to the $^4T_1$–$^6A_1$ electronic transition of manganese in a tetrahedral site. However the PL spectrum changes over time (weeks) to give a spectrum typical of the deep trap emission of CdS. SAED and XRD show both CdS and the Mn-doped CdS particles to be in the hexagonal phase. TEM and high resolution TEM show images of nanosize particles with clear lattice fringes. EPR spectra and ICP results confirm the presence of manganese in the CdS nanoparticles. EPR spectra showed that CdS : Mn was not stable over longer periods of time with segregation of manganese at the surface of particles in older samples of CdS. By contrast, the ZnS : Mn samples were quite stable for several weeks.

Introduction

The doping of manganese into II/VI semiconductor nanoparticles potentially gives a new class of materials.[1] Mn-doped ZnS and CdS quantum dots both have orange luminescence attributed to the spin forbidden $^4T_1$–$^6A_1$ electronic transition of manganese(II) in a tetrahedral site.[1–7] These properties are due to the strong exchange coupling between the localized moments of the paramagnetic dopant and the band electrons of the semiconductor. Most reports on Mn-doped ZnS and CdS nanoparticles use a colloidal route based on the simultaneous precipitation of both CdS (or ZnS) and MnS.[1–6] $Cd_{1-x}Mn_xS$ has also been synthesized by a co-precipitation reaction in reverse micelles.[7] All these studies have concluded that only a small fraction of the initial manganese added is incorporated into the crystal lattice with a large proportion of the manganese remaining on the surface or forming MnS precipitates. The location of the manganese in the dots is important as it affects optical properties. Murphy *et al.*[4] reported that manganese doped ZnS gave orange emission (585 nm) whereas the ZnS dots with manganese on the surface emit in the ultraviolet (435 nm). Recently Bawandi and co-workers[8] synthesised TOPO-capped Mn-doped CdSe using two different manganese precursors. They found that almost all of the manganese resides near the surface in the doped sample obtained by using manganese salts whereas by use of an organometallic complex $[Mn_2(\mu\text{-SeMe})_2(CO)_8]$ manganese was incorporated in the lattice. Overall they concluded that most of the manganese atoms stay in the surface layer of the lattice. The local structure of these particles has been studied by transmission electron microscopy (TEM), X-ray diffraction (XRD), energy dispersion spectroscopy (EDS), electron paramagnetic resonance (EPR) and ^{113}Cd nuclear magnetic resonance (NMR) spectroscopy.

In this paper we report the synthesis and characterization of TOPO capped Mn-doped ZnS and CdS nanoparticles using an air-stable single-source precursor, bis(diethyldithiocarbamato)-zinc(II) $[Zn(S_2CNEt_2)_2]$ and manganese dichloride for ZnS : Mn and bis(methylhexyldithiocarbamato)cadmium(II) $[Cd(S_2CNMe(^nHex))_2]$ and manganese dichloride for ZnS : Cd particles.

Experimental

Chemicals

Tri-*n*-octylphosphine oxide (TOPO), tri-*n*-octylphosphine (TOP), *n*-methylhexylamine, carbon disulfide, manganese(II) chloride and $Cd(OH)_2{\cdot}2H_2O$, were purchased from Aldrich Chemical Company Ltd and methanol, toluene from BDH. TOPO was purified by vacuum distillation at *ca.* 250 °C (0.1 Torr). The solvents were distilled, deoxygenated under a nitrogen flow and stored over molecular sieves (type 4 Å, BDH) before use. Bis(diethyldithiocarbamato)zinc(II) was purchased from Aldrich Chemical Company Ltd and was used after recrystallizing from toluene.

 DOI: 10.1039/b102709n

Synthesis

All experiments were carried out by using dry solvents and standard Schlenck techniques. Glassware was dried in the oven before use and TOPO (tri-*n*-octylphosphine oxide) was used after purification by vacuum distillation.

Preparation of $Cd(S_2CNMe(^nHex))_2$

$[Cd(S_2CNMe(^nHex))_2]$ was synthesised according to the literature method.[9] A mixture of $Cd(OH)_2{\cdot}2H_2O$ (8.43 g, 46.2 mmol), CS_2 (4.6 cm^3, 77.2 mmol) and *N*-methylhexylamine (11.6 cm^3, 76.3 mmol) in ethanol (50 cm^3) was refluxed for 1 h. The mixture was filtered to remove the solid impurities and the clear filtrate was evaporated under vacuum. The yellow solid product was recrystallized from chloroform at room temperature to give $[Cd(S_2CNMe(^nHex))_2]$ (mp 74 °C, yield: 14.11 g, 28.6 mmol, 75%).

Preparation of CdS and ZnS quantum dots

The method used was essentially as described by Trindade and O'Brien.[10,11] In a typical experiment $[Cd(S_2CNMe(^nHex))_2]$ (1.0 g) was dissolved in TOP (15 ml) and injected into hot TOPO (20 g). A decrease in temperature of 20–30 °C was observed. The solution was then allowed to stabilize at 250 °C and heated for 40 min at this temperature. The pale opalescent solution was cooled to approximately 70 °C and an excess of methanol added which led to the formation of a flocculant precipitate. The precipitate was separated by centrifugation and redispersed in toluene. ZnS nanoparticles were prepared in a similar manner but using $[Zn(S_2CNEt_2)_2]$ as precursor.

Preparation of Mn-doped ZnS or Mn-doped CdS quantum dots

In a typical experiment $Zn(S_2CNEt_2)_2$ (2.0 g) and $MnCl_2$ (6.9 mg, 1 mol%) were dissolved in TOP (15 ml). The resulting solution was then injected into hot TOPO (20 g) at 250 °C. After an initial drop in temperature to 210 °C the temperature was stabilized at 240 °C and the reaction was allowed to proceed for 40 min. The mixture was cooled to 70 °C and methanol was then added to it to flocculate the nanoparticles. After centrifugation, the supernatant solution was discarded and the pale white precipitate of nanoparticles was washed further with methanol to remove the excess TOPO, followed by dissolution in toluene. The above procedure was repeated for 3% and 5% doping, by varying the amount of $MnCl_2$.

Mn-doped CdS was prepared by the same method using $[Cd(S_2CNMe(^nHex))_2]$ (1.0 g) and $MnCl_2$ (2.56 mg, 1%) in TOP (15 ml).

Instrumentation

UV/VIS absorption spectroscopy: a Philips PU 8710 spectrophotometer was used to carry out the optical measurements of the semiconductor nanoparticles. The samples were placed in silica cuvettes (1 cm path length).

Photoluminescence spectroscopy: a Spex FluoroMax instrument with a xenon lamp (150 W) and a 152 P photomultiplier tube as a detector was used to measure the photoluminescence of the particles. Good spectral data was recorded with the slits set at 2 nm and an integration time of 1 s. The samples were quantitatively prepared by dissolving 25 mg in 10 ml toluene. The samples were placed in quartz cuvettes (1 cm path length) used as blanks for all measurements. The wavelength of excitation was set at a lower value than the onset of absorption of a particular sample.

X-Ray diffraction (XRD): X-Ray diffraction patterns were measured using a Philips PW 1700 series automated powder diffractometer using Cu-K_α radiation at 40 kV/40 mA with a secondary graphite crystal monochromator. Samples were prepared on glass slides (5 cm). A concentrated toluene solution was slowly evaporated at room temperature on a glass slide to obtain a sample for analysis.

Electron microscopy: a JEOL 2000 FX MK 1 operated at 200 kV electron microscope with an Oxford Instrument AN 10000 EDS Analyser was used for conventional TEM (transmission electron microscopy) images. Selected area electron diffraction (SAED) patterns were obtained using a JEOL 2000FX MK 2 electron microscope operated at 200 kV. The samples for TEM and SAED were prepared by placing a drop of a dilute solution of sample in toluene on a copper grid (400 mesh, agar). The excess solvent was wicked away with a paper tip and completely dried at room temperature.

Electron paramagnetic resonance (EPR): measurements were made on a Bruker 200D X-band spectrometer employing 100 kHz modulation, magnetic field markers from an NMR gaussmeter and an external microwave frequency counter.

Results and discussion

The increase in the band gap of semiconductor nanoparticles due to quantum confinement effects is widely reported.[12–15] The quantum size effects start to appear when the particle size becomes smaller than the Bohr diameter. The incorporation of manganese into the crystal lattice of nanometric semiconductors should have an effect on the optical properties. The TOPO-capped ZnS nanoparticles synthesized from $Zn(S_2CNEt_2)_2$, an air stable single source precursor, exhibit a band edge at 315 nm (3.96 eV) with an absorption shoulder at 330 nm (Fig. 1). This represents a blue shift of 0.31 eV in comparison to bulk ZnS (340 nm, 3.65 eV). The band edge of Mn-doped ZnS is at 324 nm (3.82 eV) for 1%, and is at 320 nm (3.87 eV) for 3 and 5% doped samples. The relatively small difference in the band gap of the different samples indicates a relatively narrow size distribution from the original preparation. The level of Mn-doping as measured by ICP-AES is 0.72% for the 1% sample, 1.50% for 3% and 4.62% for the 5%.

The TOPO capped CdS nanoparticles synthesized from $[Cd(S_2CNMe(^nHex))_2]$, exhibit a band edge at 475nm (2.61 eV) with a distinct excitonic shoulder at 440 nm (Fig. 2). The optical absorption spectrum of Mn-doped CdS is slightly broader than that of the equivalent parent CdS with the band edge red-shifted and at 506 nm (2.45 eV). The shoulder visible at 440 nm in CdS is smoothened out in the doped sample. This effect could be due to a slightly broader size distribution in the doped sample. The band edges of both CdS and Mn-doped CdS show blue shifts with respect to bulk CdS (512 nm, 2.42 eV) (Fig. 2).

The ZnS nanoparticles synthesized by our method are capped by TOPO and the near band edge emission (448 nm) of the nanocrystalline ZnS is slightly red shifted in relation to its absorption band edge. The PL spectra of all the Mn-doped

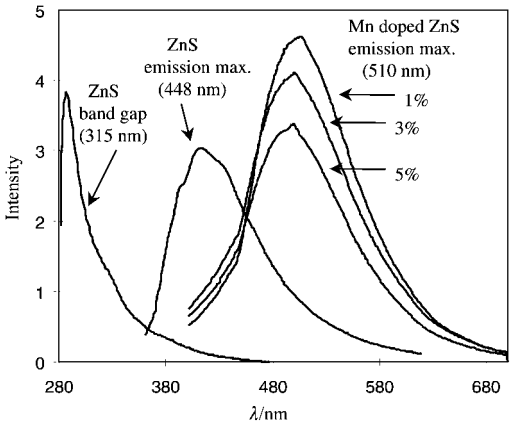

Fig. 1 Absorptiona and emission spectra of ZnS and Mn-doped ZnS.

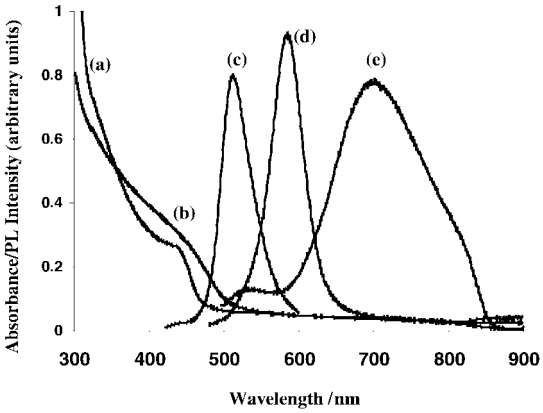

Fig. 2 Optical absorption spectra of (a) CdS and (b) Mn-doped CdS. PL spectra of (c) CdS, (d) Mn-doped CdS (fresh) and (e) Mn-doped CdS after 3 weeks.

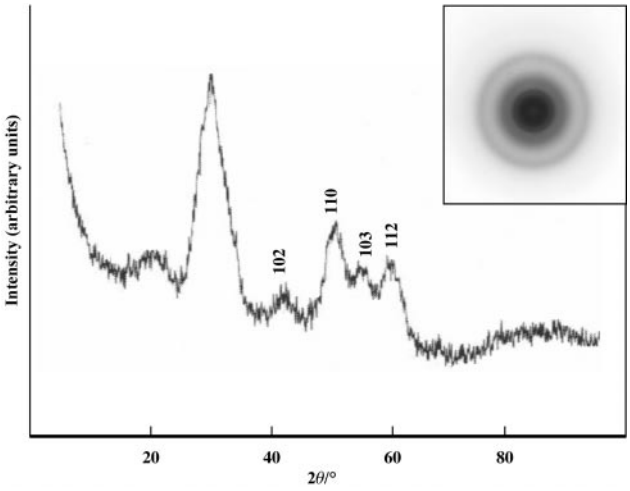

Fig. 3 The XRD and SAED pattern of Mn-doped ZnS.

ZnS samples show an emission maximum at 510 nm (λ_{ex} = 380 nm) which is *ca.* 75 nm (0.02 eV) blue shifted as compared to those reported previously at 585 nm (Fig. 1).[1–7] This blue shift appears to be caused by the smaller size of the particles. There is no change in the wavelength of emission as the level of Mn-doping changes. The 1% doped sample has the highest intensity emission peak, followed by the 3% and then the 5% sample which is consistent with the results reported by Murphy and coworkers.[4] There is a clear difference of photoluminescence intensity and emission maximum between ZnS and Mn-doped ZnS samples. However the intensity difference between the 5% Mn-doped sample and ZnS is negligible. Our PL results are considerably different to those reported by Murphy and coworkers,[4] where in all the samples emission maxima were observed at 435 and 585 nm. In our samples only one emission maximum was observed at 510 nm.

The photoluminescence spectrum of the CdS nanoparticles shows a very narrow emission bandwidth with an emission maximum at 514 nm (Fig. 2). This is consistent with previously observed photoluminescence behavior for CdS synthesized by a similar method with the emission attributed to band–band electron–hole recombination. The photoluminescence spectrum of Mn-doped CdS nanoparticles differs from that of CdS (Fig. 2). A narrow, slightly more intense spectrum is observed, with an emission maximum red shifted at 585 nm. This emission is characteristic of the manganese(II) internal $^4T_1$–$^6A_1$ transition. The absence of any deep trap emission in both the samples suggests that the surface coverage by TOPO is very efficient in the nanoparticles. However, a photoluminescence spectrum carried out on the Mn-doped sample after three weeks is remarkably different. The emission maximum is further red shifted to 705 nm, with a "hump" at 544 nm and the Mn^{2+} emission peak at 585 nm no longer present. This means that the dominant emission at 705 nm is due to recombination from the trap states. The appearance of surface traps could be due to the loss of capping agent from the nanoparticles with time as a result of their instability in solution. This suggestion is confirmed by the appearance of a fine yellow precipitate of CdS nanoparticles from the toluene solution.

The XRD pattern of the 1% Mn-doped ZnS sample shows broad peaks typical for samples in the nanosize regime which makes the distinction between the hexagonal and cubic ZnS phases difficult. However, the peaks in the diffraction pattern can be assigned to the hexagonal phase of ZnS more readily than to cubic with the (002), (110), (103) and (112) planes of the wurtzite phase being visible (Fig. 3). The selected area electron diffraction pattern exhibits broad diffuse rings typical of particles of these sizes. The (002), (110) and (112) planes were indexed confirming the hexagonal phase (Fig. 3). The TEM micrograph of the 1% sample shows particles which are monodispersed with a diameter of 3.6 nm ($\pm$5%) (Fig. 4(a)). The lattice fringes visible in the HRTEM micrograph are indicative of the crystalline nature of the particles (Fig. 4(b)).

The diffraction pattern of Mn-doped CdS also shows broad peaks typical of particles in the nanosize regime (Fig. 5). The (110), (103) and (112) planes of wurtzite CdS are clearly distinguished in the pattern (Table 1). The SAED pattern consists of broad diffuse rings again typical of small particles. The diffraction rings are indexed to the (100), (102), (103) and (112) planes so confirming the wurtzite phase. The diffraction pattern is similar to bulk CdS without any change in phase, however the (110), (103) and (112) diffractions are slightly broader in the doped sample. This effect could be as a result of the smaller size of the Mn-doped CdS particles or because of

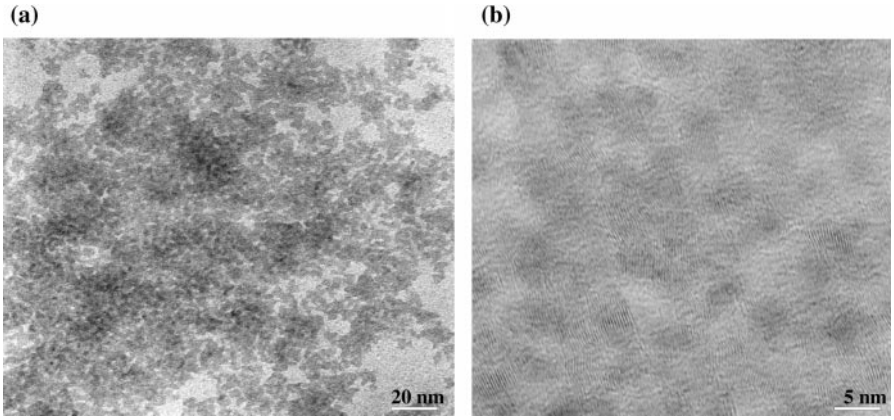

Fig. 4 TEM showing Mn-doped ZnS (0.72%) and (b) HRTEM of the same sample with particle diameter of 3.56 ($\pm$5%) nm.

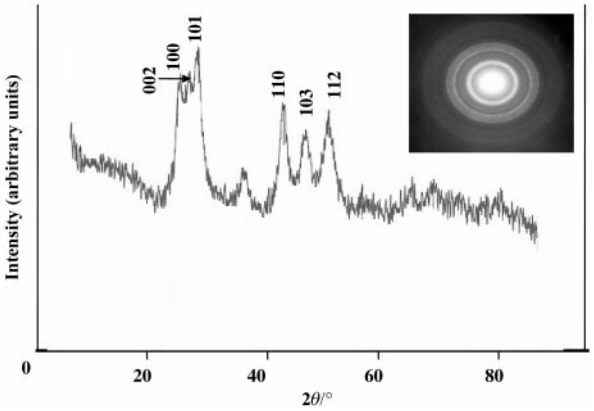

Fig. 5 The XRD and SAED pattern of Mn-doped CdS (1%).

Table 1 XRD and SAED data for the hexagonal phase of CdS : Mn nanoparticles

XRD data			SAED data	
d(exp.)/Å	*d*(lit.)/Å	*hkl*	*d*(exp.)/Å	*hkl*
3.55	3.57	100	3.60	100
3.33	3.36	002		
3.16	3.16	101	3.20	101
2.06	2.07	110		
1.90	1.90	103	1.87	103
1.76	1.76	112	1.75	112

the substitution of manganese in the sulfur sites of the CdS crystal lattice. The latter is more likely since the TEM micrographs and the absorption spectra indicate that the Mn-doped CdS particles are larger than those of CdS (Fig. 6(a)). The TEM micrograph of the Mn-doped sample shows particles with a diameter of 5.44 nm ($\pm$8%) (histogram shown in Fig. 6(b)) while the CdS nanoparticles had an average diameter of 5.12 nm ($\pm$7%). The particles appear clustered forming "islands" of particles. HRTEM shows that the particles are well defined. The lattice fringes visible in the HRTEM micrograph (Fig. 6(c)) of a single quantum dot are indicative of the crystalline nature of the particles.

The EPR spectra obtained for both the doped ZnS and CdS samples show some weak partially resolved peaks superimposed on a broad background signal. In ZnS this background signal increases at higher manganese doping (accompanied by a poorer resolution of the weak signals). The weak 6-line spectrum characteristic of the Mn^{2+} can be observed for the 1% sample (Fig. 7). The resolution was not greatly improved at low temperatures or for dilute solutions in toluene. It has been suggested that dipole–dipole interactions

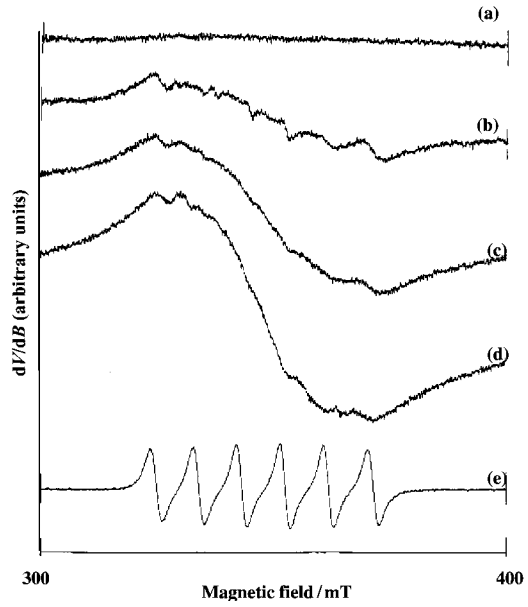

Fig. 7 Room temperature EPR spectra of Mn-doped ZnS nanoparticles: (a) undoped ZnS nanoparticles, (b) ZnS : Mn (0.72%), (c) ZnS : Mn (1.5%), (d) ZnS : Mn (4.62%), (e) standard EPR signal for Mn.

between the manganese impurities can produce a broadening which gives rise to a poor overall resolution and a broad background signal.[16] The concentrations of manganese in the ZnS as calculated from ICP and spin counting are comparable for all the levels of doping (1, 3 and 5%) (Fig. 8). The amount of manganese calculated by spin counting and ICP, as compared to the manganese input is in line with expectations in the 1% sample which shows *ca.* 80% incorporation of manganese

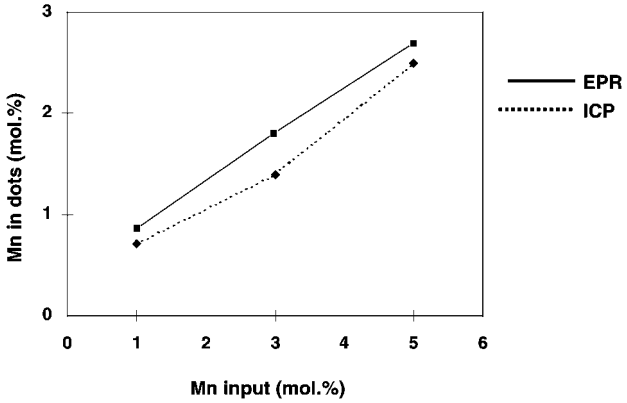

Fig. 8 A plot of percentage of Mn input *vs.* Mn found in the nanoparticles.

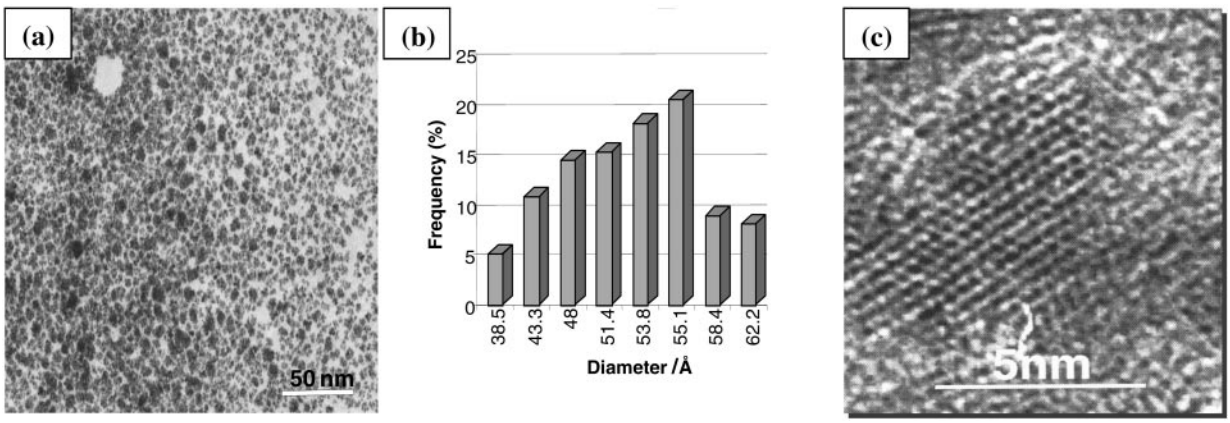

Fig. 6 (a) TEM image of Mn-doped CdS, (b) particle size distribution (diameter 5.44 ($\pm$8%) nm) and (c) HRTEM image of a single quantum dot.

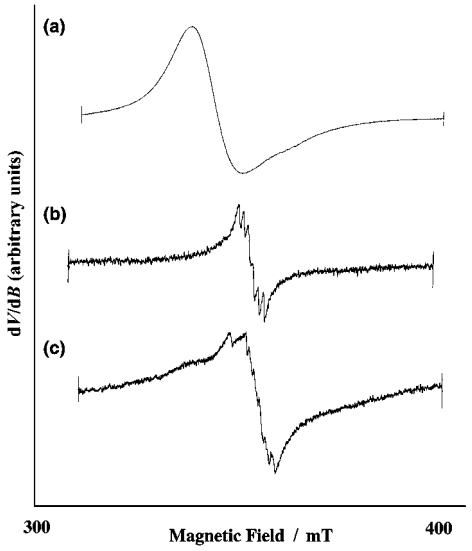

Fig. 9 EPR spectra of Mn-doped CdS as a solid (a) and as a solution in toluene (fresh) (b) and after 3 weeks (c).

whereas in the 3 and 5% samples the doping of manganese is reduced to *ca.* 50%. This observation is in agreement with previous accounts, which report inefficient (*ca.* 30%) manganese incorporation.[17]

The EPR spectrum of a fresh powdered Mn-doped CdS sample shows an intense broad signal, which could be attributed to Mn–Mn interactions (Fig. 9(a)).[1,2,6] The spectrum of a solution in toluene of the same sample shows weak partially resolved hyperfine structure superimposed on a broad background signal (Fig. 9(b)). This spectrum is characteristic of manganese(II) ions in tetrahedral sites which could be attributed to manganese incorporated into the CdS lattice. The spectrum of the solid sample taken one week later shows a remarkable decrease in the resolution of the fine structure Fig. 9(c)). This change may be due to the segregation of manganese at the surface of particles. No such change was observed in ZnS : Mn samples. The PL emission at 585 nm confirms the incorporation of manganese into the lattice. The amount of manganese present in the sample as measured by ICP-AES analysis is 0.65%, which is slightly higher when compared to previous measurements.[7,17]

It has been observed that the ZnS : Mn samples are quite stable and show no change in their PL or EPR spectra over several weeks, whereas CdS : Mn samples showed a considerable change in their EPR spectra after a week. One possible explanation of this behavior is that manganese (ionic radius = 80 pm) and zinc (ionic radius = 74 pm) have comparable ionic radii, hence the replacement of zinc by manganese will disturb the crystal lattice less than for the larger cadmium (ionic radius = 92 pm). Mn-doping in CdS or CdSe[8] is always problematic (manganese segregates at the surface of particles) as compared to ZnS[4] or ZnSe.[18]

Conclusions

Nanoparticles of CdS or ZnS and Mn-doped CdS or Mn-doped ZnS, close to monodispersed, and capped with TOPO have been prepared by a single source route using bis(diethyldithiocarbamato)zinc(II) or bis(methylhexyldithiocarbamato)-cadmium(II) and manganese dichloride. The optical properties of the Mn-doped CdS or ZnS nanoparticles differ from those of CdS or ZnS. X-Ray diffraction and electron microscopy show the particles to be nanometric in size with the hexagonal phase dominant.

Photoluminescence measurements show emission maxima at 448 nm for ZnS and 510 nm for ZnS : Mn samples. Doped samples give varying intensity of emission depending on the concentration of manganese in the sample; the highest intensity measured for ZnS : Mn(1%) samples and the lowest for ZnS : Mn(5%). Selected area electron diffraction (SAED), X-ray diffraction (XRD) and transmission electron microscopy (TEM) show the material to be of the hexagonal phase. High resolution transmission electron microscopy (HRTEM) showed well-defined images of nanosize particles with clear lattice fringes. EPR spectra and ICP results confirm the presence of manganese in ZnS quantum dots and also correspond to the amount of manganese in each ZnS sample

The PL spectrum of the doped Mn-doped CdS nanoparticles gives an emission maximum at 585 nm. SAED and XRD show both CdS and the Mn-doped CdS particles to be of the hexagonal phase. EPR spectra and ICP results confirm the presence of manganese in the CdS nanoparticles.

EPR spectra showed that CdS : Mn was not stable over longer periods of time resulting in the segregation of manganese at the surface of particles in older samples of CdS whereas the ZnS : Mn samples were quite stable for several weeks.

Acknowledgements

We thank the Royal Society and the National Research Foundation (NRF) for support to N. R. and a program of collaboration between UZULU and ICSTM. P. O'B. thanks the EPSRC for a grant. P. O'B. is the Sumitomo/STS visiting Professor of Materials Chemistry at IC. We also thank Dr A. D. Oduwole (QMW) for the EPR spectroscopy.

References

1 R. N. Bhargava, D. Gallagher and A. Nurmikko, *Phys. Rev. Lett.*, 1994, **72**, 416.
2 D. Gallagher, W. E. Heady, J. M. Racz and R. N. Bhargava, *J. Cryst. Growth*, 1994, **138**, 970.
3 Y. L. Soo, Z. H. Ming, S. W. Huang, Y. H. Kao, R. N. Bhargava and D. Gallagher, *Phys. Rev. B*, 1994, **50**, 7602.
4 K. Sooklal, B. S. Cullum, S. M. Angel and C. J. Murphy, *J. Phys. Chem.*, 1994, **100**, 4551.
5 Y. Wang, N. Herron, K. Moller and T. Bein, *Solid State Commun.*, 1991, **77**, 33.
6 L. Levy, N. Feltin, D. Ingert and M. P. Pileni, *J. Phys. Chem. B*, 1997, **101**, 9153.
7 G. Counio, T. Gacoin and J. P. Boilot, *J. Phys. Chem. B*, 1998, **102**, 5237.
8 F. V. Mikulec, M. Kanu, M. Bennati, D. A. Hall, R. G. Griffin and M. G. Bawandi, *J. Am. Chem. Soc.*, 2000, **122**, 2532.
9 P. O'Brien, D. J. Otway and J. R. Walsh, *Adv. Mater., Chem. Vap. Deposit.*, 1997, **3**, 227.
10 T. Trindade and P. O'Brien, *Adv. Mater.*, 1996, **8**, 161.
11 T. Trindade and P. O'Brien, *Chem. Mater.*, 1997, **9**, 523.
12 D. Duongong, J. Ramsden and M. Gratzel, *J. Am. Chem. Soc.*, 1982, **104**, 2977.
13 R. Rossetti, J. L. Ellison, J. M. Gibson and L. E. Brus, *J. Chem. Phys.*, 1999, **80**, 4464.
14 A. Henglein, *Chem. Rev.*, 1989, **89**, 1861.
15 M. L. Steigerwald and L. E. Brus, *Acc. Chem. Rev.*, 1990, **23**, 183.
16 B. Ludolph, M. A. Malik, P. O'Brien and N. Revaprasadu, *Chem. Commun.*, 1998, 1849.
17 L. Levy, J. F. Hochepied and M. P. Pileni, *J. Phys. Chem.*, 1996, **100**, 18322.
18 D. J. Norris, N. Yao, F. T. Charnock and T. A. Kennedy, *Am. Chem. Soc. Nano Lett.*, 2001, **1**(1), 3.